Uncertainty Assessment Framework for IGBT Lifetime Models. A Case Study of Solder-Free Modules

Ander Zubizarreta[1], Markel Penalba[1,4], David Garrido[1], Unai Markina[2], Xabier Ibarrola[2] and Jose I. Aizpurua[3,4]*

[1] *Mondragon University, Mondragon, 20500, Spain*
ander.zubizarreta@alumni.mondragon.edu
mpenalba@mondragon.edu
dgarrido@mondragon.edu

[2] *Ingeteam, Zamudio, 48170, Spain*
unai.markina@ingeteam.com
xabier.ibarrola@ingeteam.com

[3] *University of the Basque Country (UPV/EHU), Faculty of Computer Science, Donostia - San Sebastian, 20018, Spain*
**Corresponding author: joxe.aizpurua@ehu.eus*

[4] *Ikerbasque – Basque Foundation for Science, Bilbao, 48009, Spain*

ABSTRACT

Insulated gate bipolar transistors (IGBTs) are ubiquitous semiconductor devices used in diverse electronic power applications. The reliability and lifetime assessment of IGBTs is intricate and influenced by different ageing processes. One of the main ageing mechanisms is the bond wire lift-off failure mode. The model used to describe this failure mode and estimate the IGBT lifetime is influenced by different variables and factors, which are stochastic, and tend to be specifically adjusted for different IGBT modules and applications. However, unless these variables are not assessed with respect to potential sources of uncertainty, the IGBT lifetime estimate leads to a single-value deterministic estimate, which, frequently, results inaccurate. In this context, assessing the influence of the variability of these variables on the lifetime model is a crucial activity for an uncertainty-aware IGBT lifetime estimate and adoption of appropriate sensing technology. Accordingly, this paper presents a methodology to evaluate the impact of the uncertainty of IGBT lifetime parameters on the lifetime estimate. The approach is first validated on three different experimental IGBT operation profiles, demonstrating the impact of variations of certain variables on the damage estimation. The approach has been tested here for a single lifetime model, but it is generally applicable to other IGBT lifetime models.

1. INTRODUCTION

Insulated Gate Bipolar Transistors (IGBTs) are semiconductor devices used in power electronic converters for different applications, ranging from low-power IGBTs used in few kilowatts applications like induction cookers to high-power IGBT modules for megawatts converters used in renewable energy plants, such as photovoltaic and wind farms (Lutz, Schlangenotto, Scheuermann, & De Doncker, 2018). IGBTs are used as electronic switches due to their high-efficiency and fast-switching properties (Elwakeel et al., 2023). However, they are often ranked as having the lowest reliability in power converters (Yang et al., 2010). Recently, the growing interest in amortizing the initial capital investment of renewable energy plants and reducing their operational costs through predictive maintenance has led to an extensive interest and research focused on prognostics & health management (PHM) applications, specially focused on the lifetime assessment of IGBT-based power modules (Degrenne, Kawahara, & Mollov, 2015; Abuelnaga, Narimani, & Bahman, 2021; Fu, Peyghami, Núñez, Blaabjerg, & De Schutter, 2023; Cai, Zhao, Ma, & Zhou, 2020).

The main failure modes of IGBTs can be classified into sudden and ageing failures (Abuelnaga et al., 2021). Sudden failures are caused by random phenomena, such as cosmic radiation or electric discharge. In contrast, ageing failures are

Ander Zubizarreta et al. This is an open-access article distributed under the terms of the Creative Commons Attribution 3.0 United States License, which permits unrestricted use, distribution, and reproduction in any medium, provided the original author and source are credited.
https://doi.org/10.36001/IJPHM.2025.v16i1.4164

caused by environmental or operational stress, which overcome a failure threshold limit.

The main ageing failure causes of IGBTs are classified into corrosion, electric migration, dielectric breakdown and fatigue (Lutz et al., 2018). The focus of this work is on fatigue damage, which is caused by an imbalanced coefficient of thermal expansion (CTE) of the different materials within the IGBT structure. Figure 1 shows a schematic view of the internal lateral structure of an IGBT module and its materials.

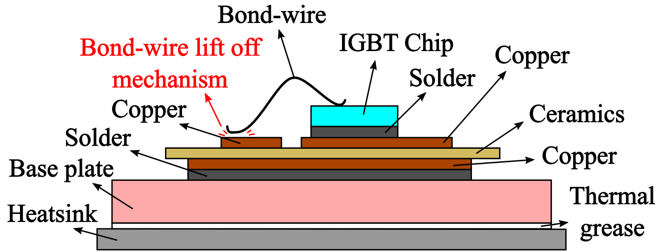

Figure 1. Structure of IGBT module divided by layers indicating bond wire lift-off mechanism — adapted from (Hernes et al., 2021).

IGBTs operate in switching mode with different working power profiles, which leads to repeated temperature oscillations that cause damage in the joints of different material layers as they have different CTEs. In turn, this damage is expressed mainly as solder cracking failure modes (Lutz et al., 2018) and bond wire lift-off (cf. Figure 1).

1.1. Motivation

The degradation of IGBTs can be measured directly using expensive laboratory instrumentation, e.g. 3D x-rays (Yaqub, Li, & Johnson, 2015), or indirectly, using internal chips where temperature is modelled through the virtual junction temperature, T_j (Degrenne et al., 2015; Degrenne, Ewanchuk, David, Boldyrjew, & Mollov, 2019). The junction temperature increases as the current path area decreases due to the bond wire lift-off phenomenon (Tu et al., 2022; Y. Huang, Luo, Xiao, Liu, & Tang, 2023). The direct measurement of T_j is not feasible because the inside of the chip is not reachable. Accordingly, in order to monitor the fault-to-failure progression, it is needed to track different failure precursors, called temperature-sensitive electrical parameters (TSEPs) (Degrenne et al., 2019). These TSEPs have predefined temperature dependencies, and they can be directly measured from the gate-emitter circuit or collector-emitter circuit in order to determine T_j. Mandeya *et. al* compare several TSEPs for a given IGBT module, showing where the sensor is placed, when the measurement is performed and, finally, which sensor type is required for each TSEP (Mandeya, Chen, Pickert, & Naayagi, 2018). Focusing on the bond wire lift-off failure mode, the most widely used TSEP is the collector-emitter voltage, $V_{CE(on)}$. As the bond wires age, the equivalent conduction resistance increases and this leads to increasing the $V_{CE(on)}$.

There are pre-defined threshold values for TSEPs, which define end-of-life limits, e.g. 5% increase of $V_{CE(on)}$ with respect to initial conditions (Abuelnaga et al., 2021). Figure 2 shows the output characteristics of an IGBT collector-emitter voltage during the conduction phase of the IGBT, $V_{CE(on)}$, as a function of conduction currents, $I_{C(on)}$. It can be observed that it is directly related with temperature, from $25°C$ to $150°C$.

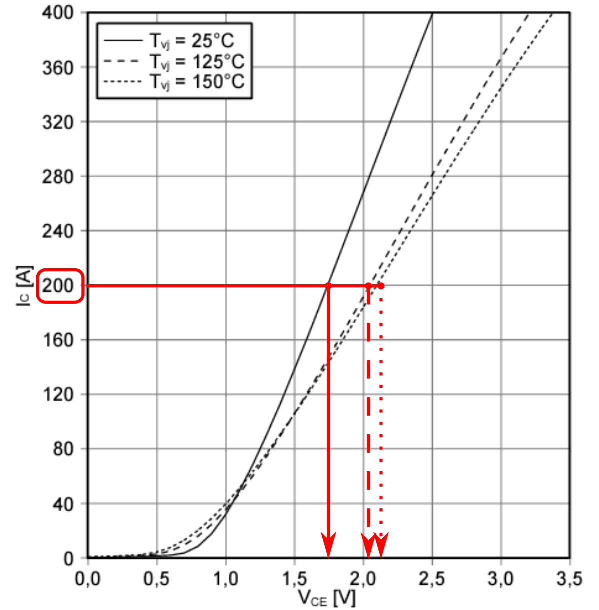

Figure 2. IGBT data from Infineon's manufacturer datasheet (Infineon Technologies AG, 2013).

However, TSEP measurements are prone to errors and uncertainties due to the measurement resolution of probes and circuits. For example, high voltage withstand is needed during blocking state of the IGBT, yielding to a low-resolution during conduction state. In addition, current measurements are needed because $V_{CE(on)}$ depends on $I_{C(on)}$, as shown in Figure 2. A characterization of each IGBT is needed, even for the same IGBT reference, as is highlighted in bold font in Table. 1, where disparity of $V_{CE(on)}$ values can be observed for the same temperature and current value using the same manufacturer IGBT reference.

Table 1. Collector-emitter saturation voltage values (Infineon Technologies AG, 2013).

I_c **[A]**	V_{GE} **[V]**	T_{vj} **[°C]**	$V_{CE,sat}$ **[V]**
200	15	25	**Typical = 1.75, Maximum = 2.15**
		125	Typical = 2.05
		150	Typical = 2.1

In this context, the lifetime modelling process for the bond wire lift-off failure mode of IGBTs focuses on the estimation

of the remaining number of cycles as a function of junction temperature profiles, among other parameters that influence the degradation (Abuelnaga et al., 2021).

The junction temperature (T_j) profile estimation has a direct dependency on the data acquisition of TSEPs and related measurements. Mainly on the $V_{CE(on)}$, but also on other measurements like $I_{C(on)}$, case temperature (T_c) and ambient temperature (T_a). Note that the T_c and T_a can only be considered if heatsink is characterized for the bond wire lift-off failure mode. As a consequence, these measurements are prone to different sources of uncertainty and measurement errors. From the junction temperature, the associated thermal cycles are estimated, ΔT_j, which are processed through cycle counting methods. Again, the relationship between the measurement errors and uncertainties is accentuated due to the post-processing applied to the T_j signal. Figure 3 shows the functional relationship between precursor-tracking experiments, measurements, processing activities including lifetime influencing variable estimation, and lifetime modelling activities.

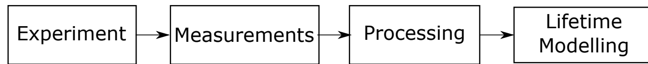

Figure 3. Conceptual block diagram showing relation between precursors, experimentation and lifetime modelling.

1.2. Related Work

Different IGBT lifetime models for bond wire lift-off failure mode assessment have been proposed and evaluated in the literature (Abuelnaga et al., 2021). Due to the lack of accuracy and consistency of the obtained IGBT lifetime estimates, there have been proposed extensions and variations for specific contexts and applications. For example, Hernes *et al.* evaluated the IGBT lifetime at low temperature stress cycles (Hernes et al., 2021). Huang and Mawby presented a lifetime estimation model for die-attach solder fatigue through Weibull-based curve fitting adjusted on the accelerated ageing tests (H. Huang & Mawby, 2013), which is subsequently connected with the damage model to estimate the IGBT lifetime. Yizhou *et al.* presented a lifetime estimation approach using a Bayesian estimation approach combining Coffin-Manson models with finite element simulations (Lu & Christou, 2017). Fei *et al.* developed a novel IGBT lifetime prediction model based on the collector-emitter on-resistance (Qin et al., 2021). Haque *et al.* presented a remaining useful life (RUL) assessment method based on tracking the evolution of $V_{CE(on)}$ and estimating the time to reach a voltage limit (Haque, Choi, & Baek, 2018). Astigarraga evaluated the implementation of Prognostics and Health Management (PHM) technologies for IGBT RUL estimation for electric vehicle applications (Trespaderne, 2016).

With the proliferation of data-driven intelligent solutions, different machine-learning based health-state estimation methods have been proposed. In this direction, for example, Jiaqi *et al.* presented an IGBT health assessment approach based on machine learning methods, through health-state diagnostics based on accelerated ageing tests (J. Liu, Li, Chen, & Liu, 2022). Similarly, Rigamonti *et al.* used an unsupervised learning strategy to diagnose the health state of IGBTs based on an experimental dataset which includes collector-emitter voltage, case temperature and current measurements.

In general, it can be observed that existing IGBT lifetime estimation models and their applications do not account for the inherent sources of uncertainty in the lifetime estimation process (Antonopoulos, D'Arco, Hernes, & Peftitsis, 2021). There are exceptions that consider the uncertainty associated with the thermal modeling process through curve fitting strategies (H. Huang & Mawby, 2013), however, the different sources of uncertainty are not modeled and propagated to the damage estimation result to assess their impact on the lifetime estimation error. However, this is an important stage for the lifetime assessment of IGBT, as it is surrounded by different sources of uncertainty, and this assessment supports the health assessment under uncertainty (Changcong, Mengyao, Haodong, & Fei, 2021).

1.3. Contribution & Organization

Accordingly, the contribution of this research is the development of a damage uncertainty assessment methodology for IGBTs including different sources of uncertainty and determination of the influence of the error of different parameters on the IGBT lifetime estimation error. That is, the novelty of the work lies in the analysis of the explicit propagation of errors across lifetime estimation stages, and the quantification of its impact on lifetime estimation.

Lifetime model parameters are derived from device degradation experiments through a data fitting process. The parameter calculation is then directly dependent on the adjusted model. In this context, independent of the fitted variable values, the proposed approach provides a methodology to evaluate the impact of variables on the lifetime. The proposed approach estimates relative error values dependent on the structure of the model, not absolute values of variables. Therefore, it can be adapted to different device degradation experiments. Obtained results have broader implications for sensing and measurement equipment, as an explicit relation is obtained between the individual parameter uncertainty and overall lifetime uncertainty. The proposed framework can be used to weigh the impact of measurement technology improvements with respect to the lifetime estimation accuracy.

The remainder of this article is organized as follows. Section 2 reviews IGBT lifetime modelling methods. Section 3 presents the proposed sensitivity and lifetime assessment approach. Section 4 defines the case study. Section 5 presents

Table 2. Synthesis of IGBT lifetime models for different applications.

Model	Failure Modes	Variables	Precursors	Context	Limitations	Refs.
LESIT — Eq. (2)	Bond wire lift-off	$\Delta T_j, T_{j,m}$	V_{CE}	Al2o3	t_{ON} not considered	(Held, Jacob, Nicoletti, Scacco, & Poech, 1997; Hernes et al., 2021)
SKiM63 — Eq. (3)	Bond wire lift-off	$\Delta T_j, T_{j,m}, t_{on}, f_{diode}$	V_{CE}	Solder-free modules	Only solder-free	(Scheuermann & Schmidt, 2013)
CIPS2008 — Eq. (4)	Bond wire lift-off, Solder fatigue	$\Delta T_j, T_{j,min}, t_{on}, I, V, D$	V_{CE}	Al2o3	Applicable in the test range	(Bayerer, Herrmann, Licht, Lutz, & Feller, 2008; Hernes et al., 2021; Antonopoulos, D'Arco, Hernes, & Peftitsis, 2019)

an extensive discussion, and finally, Section 6 concludes.

2. IGBT LIFETIME MODELLING

IGBT lifetime modelling is largely based on field experience and available datasets collected over a long period of time for different IGBT technologies (Lutz et al., 2018). IGBT lifetime is generally expressed in the form of number of remaining cycles, N_f, and lifetime modelling approaches are inspired from the Coffin-Manson empirical model (IEC, 2019):

$$N_f = a\Delta T^{-n} \tag{1}$$

where a and n are empirical parameters obtained from experimental tests, and ΔT is the temperature cycle.

A well-known and widely used model is the LESIT model introduced by Held *et al.* (Held et al., 1997). In this work a number of different modules were employed with Al2O3 ceramics leading to the estimation of N_f as a function of the mean junction temperature (Held et al., 1997):

$$N_{fi} = A\Delta T_j^{\alpha}.e^{\frac{E_a}{k_B(T_{j,m})}} \tag{2}$$

where A and α are constant model parameters, k_B is the Boltzmann's constant (1.38x10^{-}23 J/K), E_a is the activation energy, ΔT_j is the junction temperature variation, and $T_{j,m}$ is the mean junction temperature.

The LESIT model in Eq. (2) has been extended for different modules and applications. As the junction temperature T_j has a direct dependency on the activation time, t_{on}, which is caused by the transient response of T_j, the present study uses validated empirical models which integrate activation time information.

Namely, the lifetime model defined by Semikron is considered (Scheuermann & Schmidt, 2013), known as SKiM63 lifetime model, which is designed for skim modules, *i.e.* a module without solder and baseplate, and an improved geometry for the wire bonds. This isolates the occurrence of the bond wire lift-off failure mode. The model includes additional factors to the Eq. (2):

$$N_{fi} = A\Delta T_j^{-\alpha} e^{\frac{E_a}{k_B T_{j,max}}} ar^{\beta_1 \Delta T_j + \beta_0} (\frac{c + t_{on}^{\gamma}}{c+1}) f_{diode} \tag{3}$$

where A is a constant scaling factor as defined immediately above, t_{on} is the activation time [s], ar is a geometry parameter defined as the bond wire aspect ratio, f_{diode} is the effect of the width difference between IGBT and diode, $T_{j,max}$ is the maximum junction temperature, c is a constant model parameter, and γ, β_0 and β_1 are additional constant model parameters determined through experimentation and parameter fitting process (Scheuermann & Schmidt, 2013).

There are other lifetime models, such as the CIPS 2008 model, which includes additional testing parameters (Bayerer et al., 2008):

$$N_{fi} = K\Delta T_j^{-\beta_1} e^{(\frac{\beta_2}{T_{j,min}+273})} t_{on}^{\beta_3} I^{\beta_4} V^{\beta_5} D^{\beta_6} \tag{4}$$

where K is a constant model parameter, I is the wire current, V is the breakage voltage, D is the bond wire diameter and $\{\beta_1, \ldots, \beta_6\}$ are fitting constants as defined immediately above.

Table 2 synthesizes the main lifetime models, their failure modes, considered variables, precursors, application context, limitations, and application reference examples (Abuelnaga et al., 2021).

From Table 2 it can be observed that there are different parameters that have been fitted to adjust the lifetime models. However, to the best of authors' knowledge, the uncertainty of these parameters and their impact on lifetime estimation has not been evaluated. Parameter-specific uncertainty information can be used to adapt experimentation activities, e.g. reduction of uncertainty through improving measuring equipment, and improve health monitoring and lifetime assessment activities. Therefore, the focus of this paper is on the uncertainty assessment of the SKiM63 model.

3. IGBT LIFETIME ASSESSMENT APPROACH

Figure 4 shows the classical IGBT lifetime assessment approach. The process starts from the `power loss` model, which calculates the losses of the IGBT module from the input loading data, and through a `thermal model` calculates the corresponding junction temperature, T_j.

The `cycle count` module estimates damage cycles, ΔT through the application of the rainflow algorithm (ASTM, 2017). The rainflow counting algorithm is a fundamental

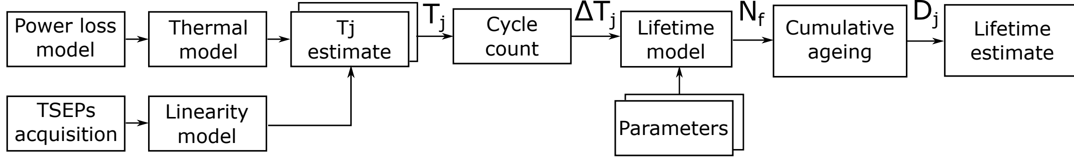

Figure 4. Classical IGBT lifetime assessment approach block diagram.

method in fatigue analysis, applied to evaluate the effects of complex loading patterns on material durability (Matsuishi, 1968). Inspired by how rain flows down a pagoda roof, this approach breaks down a load sequence into distinct stress ranges with corresponding cycle counts. By assessing stress levels and cycle durations, it quantifies the fatigue impact of each loading cycle, enabling accurate predictions of material degradation under variable-amplitude loading.

Subsequently, the remaining number of cycles, N_f is estimated from the `lifetime model` and its corresponding `parameters`. Finally, damage D_j is estimated through the Miner's `cumulative damage` law, which considers the stress contribution of each cycle to the total damage, and it is linearly accumulated as follows (Miner, 1945):

$$D = \sum_{i=1}^{J} \frac{n_i}{N_{f_i}} \tag{5}$$

where J is the total number of cycles, n_i is the identified thermal cycles, and N_{f_i} is the total number of cycles calculated through empirical lifetime modes.

3.1. Uncertainty Assessment Approach

The classical lifetime assessment approach described in Figure 4, however, does not consider sources of uncertainty. Accordingly, the main contribution of the proposed lifetime assessment approach is the integration of different sources of uncertainty, which impact on the damage estimation, such as the thermal estimate, T_j, and lifetime model parameters.

Accordingly, in order to estimate the impact of the error of different parameters on the lifetime (damage) estimate, Figure 5 shows the flowchart of the proposed uncertainty assessment approach.

The proposed framework starts from junction temperature estimate T_j and integrates different sources of uncertainty, highlighted in red in Figure 5. On the one hand, uncertainties of junction temperature values are considered, modelling the variance and errors associated with the junction temperature estimation. Errors on T_j are propagated through subsequent analysis stages, including the cycle count, lifetime model, cumulative ageing and lifetime (damage) estimation stages.

This is characterized by adding an error term (Aizpurua et al., 2019, 2021), defined as follows:

$$T_j(t) = T_j(t) + e_{T_j}(t) = T_j(t) + T_j(t) \times p \tag{6}$$

where $e_{T_j}(t)$ is the considered error term at instant t and p is the error percentage.

This error modelling strategy enables controlling the input uncertainty of a process and evaluating the impact on the output of the process. It is true that interactions among variables are not captured with this modelling process. However, this rationale enables the integration of specific errors, e.g. measurement errors due to calibration or quantization, and their impact on the process outcome.

Figure 6 shows the junction temperature error example for different error values on T_j.

The obtained junction temperature estimate including uncertainties is subsequently propagated to the cycle count algorithm, quantifying the cycle range and its impact through the rainflow algorithm. That is, it is subsequently converted into ΔT versus cycles through post-processing with the rainflow algorithm including the considered error terms. Note that this step, enables the step-wise error propagation throughout the lifetime estimation process, instead of simply adding error terms to late stages after calculating ΔT.

As for the uncertainty surrounding lifetime model variables, this is considered by redefining the lifetime equations including the corresponding error terms, which is modelled as parameter uncertainty in Figure 5. Note that the parameter uncertainty is directly connected with the lifetime modelling stage, and therefore, compared with T_j the uncertainty modelling process is simpler.

Redefinition of Eq. (3) including error terms, is as follows:

$$N_{f_i} = (A + A_{e_A})\Delta T_j^{-\alpha+\alpha e_\alpha} e^{\frac{E_a + E_a e_{E_a}}{k_B(T_{j,m}+T_{j,m}e_{T_{j,m}})}} (ar + are_{ar})^{(\beta_1+\beta_1 e_{\beta_1})\Delta T_j + (\beta_0+\beta_0 e_{\beta_0})} \left(\frac{(c+ce_c)+(t_{on}+t_{on}e_{t_{on}})^{(\gamma+\gamma e_\gamma)}}{(c+ce_c)}\right)(f_{diode}+f_{diode}e_{f_{diode}}) \tag{7}$$

where e_A denotes error of A, e_α denotes error of α, e_{E_a} denotes error of E_a, $e_{T_{j,m}}$ denotes error of $T_{j,m}$, e_{ar} denotes error of ar, e_{β_1} denotes error of β_1, e_{β_0} denotes error of β_0, e_c denotes error of c, $e_{t_{on}}$ denotes error of t_{on}, $e_{f_{diode}}$ denotes

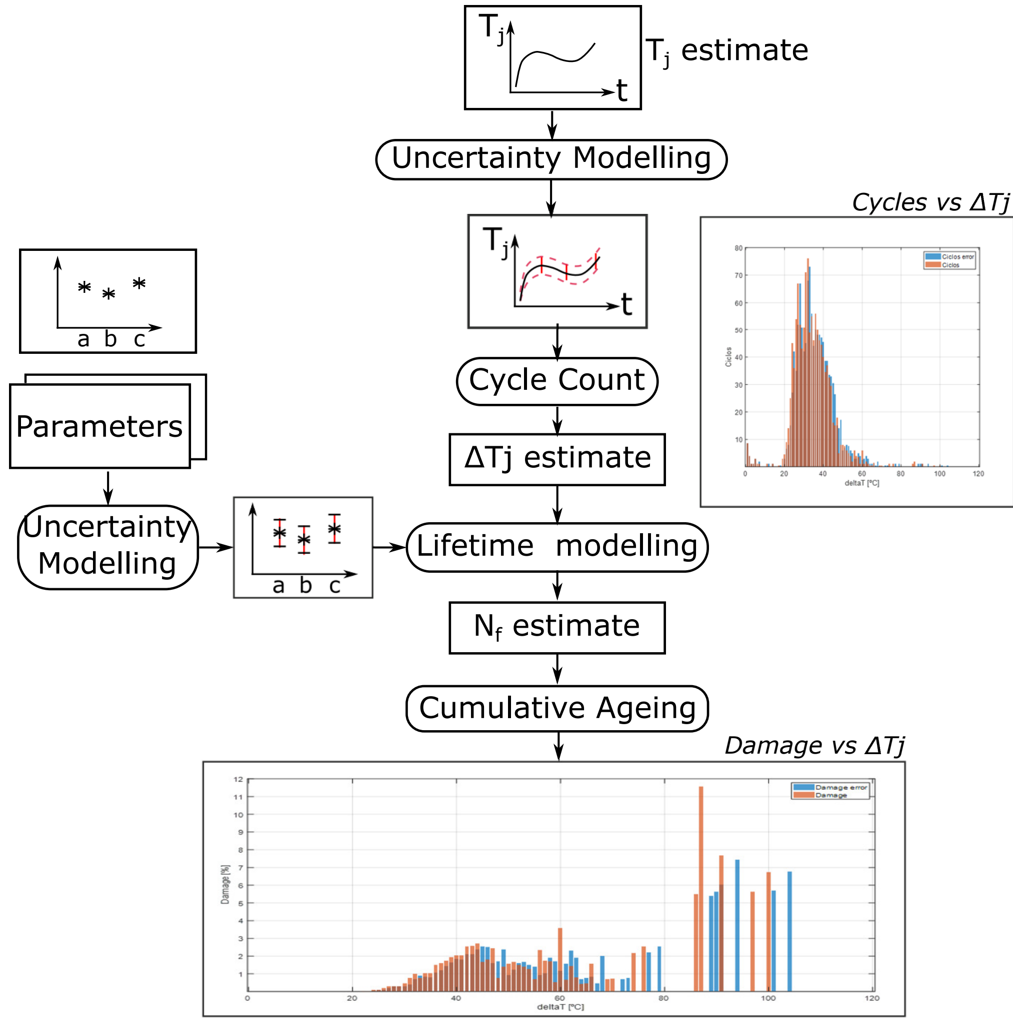

Figure 5. Flowchart of the proposed uncertainty assessment approach for IGBT lifetime assessment.

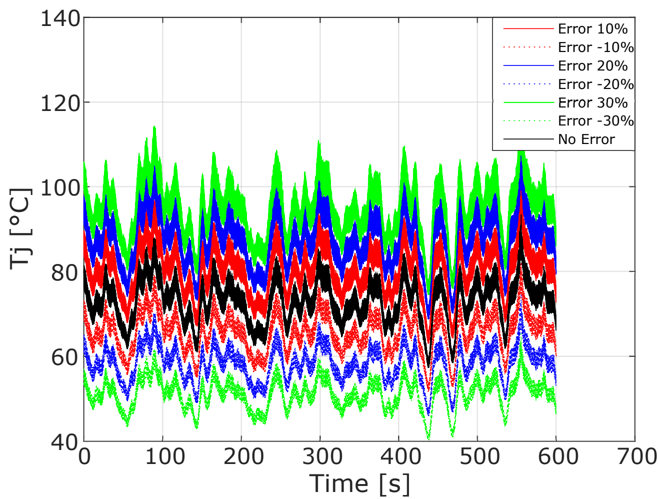

Figure 6. Error modelling example on the junction temperature.

error of f_{diode}.

Subsequently, the estimate of the number of remaining cycles, N_f, is obtained which is converted into damage cycles via cumulative ageing defined in Eq. (5).

Finally, in order to compare lifetime estimation models for damage models without uncertainty, D, and with uncertainty, D_e, the error on the damage estimate is calculated as the ratio between the damage without errors [cf. Eq. (5)] and the damage with error:

$$e_D = D_e/D \tag{8}$$

For example, e_D=0.5 would mean that there is an underestimation error of 50%, while e_D=1.5 would mean that there is an overestimation error of 50%. This ratio enables the quick comparison with respect to the model without errors and identification of underestimation or overestimation errors.

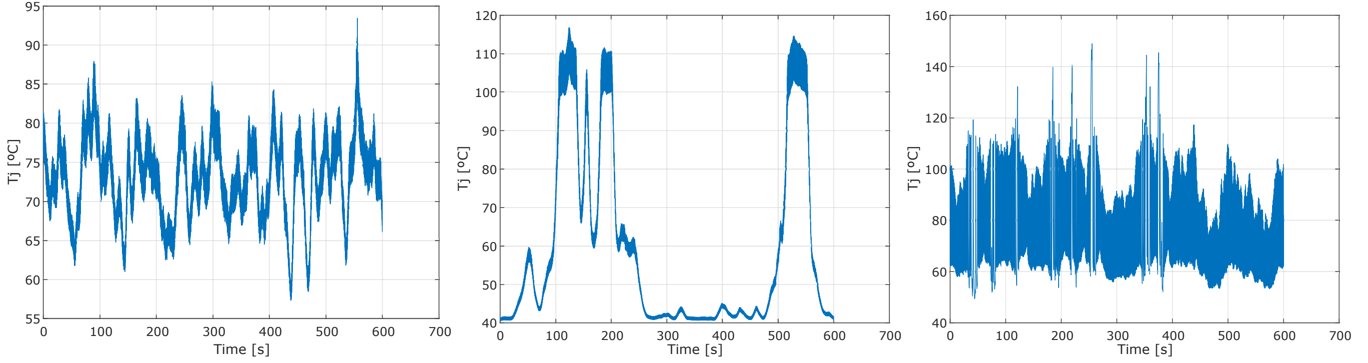

Figure 8. Junction temperature profiles, numbered #1, #2 and #3, from left to right.

Accordingly, the main objective of the proposed framework is the evaluation of the influence of different errors on the IGBT damage estimation. This information is crucial to understand the influence of parameters on damage estimation and infer their relevance for the lifetime estimation process.

4. CASE STUDY

Three different junction temperature profiles have been tested in three different scenarios, which have been obtained from monitoring the corresponding precursors and post-processing through a power loss model developed for the IGBT under study.

Figure 7 shows the workflow of the junction temperature profile conversion. The process starts with the `operation profiles` as inputs, which can correspond to different power electronic applications, and it is connected to the `grid & machine models`, which include parameters of the grid and the corresponding machine, e.g. wind turbines for wind energy applications. This is then fed into the `control & modulations` block, which includes a detailed description of the converter. Subsequently, this is connected with the `power loss` and `thermal models`, that using electrical and thermal characterizations, calculate power and thermal losses, respectively.

Figure 7. Operation profile to junction temperature profile conversion workflow.

The outcome of the process is the junction temperature, $T_j(t)$. Figure 8 shows the three junction temperature profiles assessed in this research, which show considerably different thermal properties, providing a comprehensive case study for the suggested lifetime models. These profiles have been provided by an industrial partner and were deliberately selected to assess the impact on uncertainty of diverse junction temperature profiles, with low, mild and high thermal cycles. They reflect different IGBT operation settings, including normal and extreme operation environments.

It can be observed that the temperature profile #1 includes different temperature variations, with temperature values below 100 °C. In contrast, temperature profile #2 shows fewer variations in temperature, although it has peaks above 100 °C. Finally, the temperature profile #3 includes periods of highest junction temperature with temperatures above 100 °C.

4.1. Damage Assessment

Using the damage estimation process explained in Section 3, firstly the junction temperature is post-processed through the rainflow algorithm. Figure 9 shows the cycle counting algorithm outcome for the junction temperature profile #3.

Figure 9 shows the number of cycles per cycle range (ΔT) and cycle average ($T_{j,m}$). The algorithm also provides the bounds of each cycle so that it is possible to post-process and infer activation times (t_{ON}) for lifetime estimation purposes.

Subsequently, the deterministic damage assessment is implemented using lifetime equations and corresponding parameters and temperature values. Figure 10 shows the damage assessment results obtained with the following constant values (Scheuermann & Schmidt, 2013): A=3.4368e14, α=-4.923, E_a=6.606e-2, β_1=-9.012e-3, β_0=1.942, C=1.434, γ =-1.208, f_{diode}=0.6204, k_b=8.6173e-5 and ar=0.31. Firstly, the load profile is passed through the rainflow algorithm and load cycles are estimated, Δt. Then, the damage estimation is calculated from Eq. (3) using T_j, and previously defined constants. Finally, the cumulative damage is calculated via Eq. (5).

It can be observed that the damage profile is different for different junction temperature profiles. Namely, thermal cycles (ΔT) are located below 50 °C for profile #1, above 50 °C for #2, and around 100 °C for #3. Table 3 displays the total damage estimate based upon the SKiM63 lifetime model [cf. Eq. (5)] and consumed life, assuming that a damage value of 1 would mean end of life.

It can be observed that the profile #3 causes the most damage and profile #1 causes the least. From Figure 10, comparing

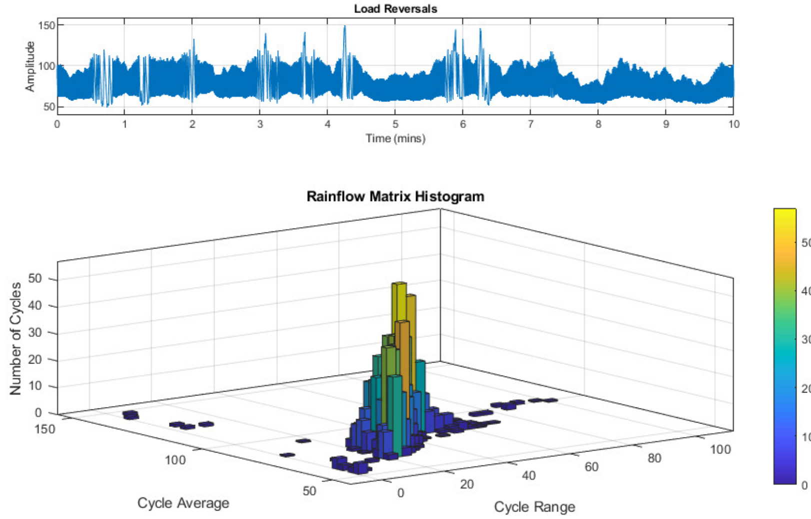

Figure 9. Rainflow algorithm outcome for the profile #3 — cf. Figure 8 right.

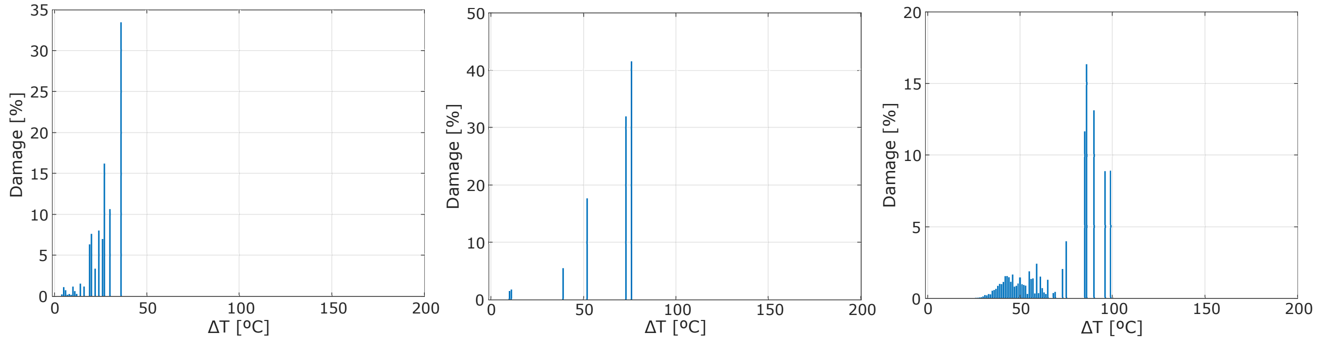

Figure 10. Damage using the lifetime model in (3) for the profiles #1, #2 and #3 in Figure 8.

Table 3. Damage estimate for the SKiM63 lifetime model.

Name	Damage	Consumed life
Profile #1	1.4123e-10	1.4123e-08%
Profile #2	9.0391e-09	9.0391e-07%
Profile #3	4.5613e-07	4.5613e-05%

profile #1 with #2, it can be observed that high temperature cycles cause more damage than low temperature cycles.

4.2. Uncertainty Assessment

The main goal of this research is not the precise lifetime estimation. Instead, the main interest and contribution of this work is on the uncertainty assessment of lifetime estimation parameters. Accordingly, the estimated lifetime values are now post-processed and compared with variations of input parameters to evaluate their impact on lifetime.

An extended range of possible error values are assessed to examine the impact on damage estimation error. Although the adopted error range may be excessive for certain sources of uncertainty, this is a deliberate decision to examine the impact of errors in different scales.

Based on the similar structure of different lifetime models in Eqs. (1)-(4), the main focus of the uncertainty assessment is on junction temperature T_j, activation time t_{ON}, and key constant parameters such as A and α, which are common to the different lifetime models.

4.2.1. Junction Temperature Uncertainty

Focusing on the uncertainty assessment of the junction temperature, a constant error has been added to each point of the signal so that the original signal is not modified and the desired controlled error is added (cf. Figure 6). Note that the modified T_j signal is first processed through the rainflow cycle count algorithm, and subsequently, the SKiM63 lifetime model is applied by propagating the error of the T_j, and quantifying the effect on damage estimation. This impact is then divided with respect to the damage without error, and the dif-

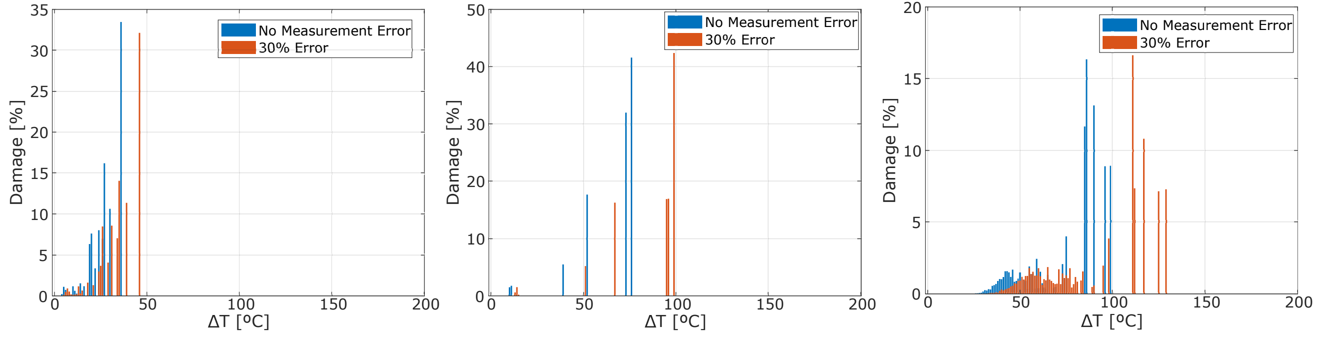

Figure 12. Impact of the error of T_j on damage assessment for the profiles #1, #2 and #3 shown in Figure 8.

ference is quantified as illustrated in Figure 10 for each profile. Additionally, Figure 11 shows the effect of the junction temperature error on the damage estimation.

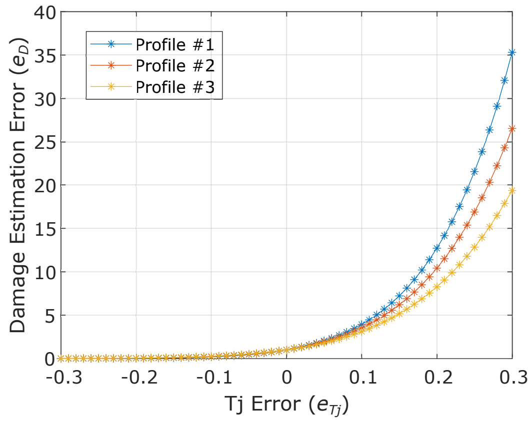

Figure 11. Effect of junction temperature error (e_{T_j}) on damage estimation error (e_D).

It can be observed in Figure 11 that the damage model is very sensitive to the errors made in junction temperature estimations. Note that the T_j affects directly the N_f calculation, but also it impacts on the cycle count ΔT.

In fact, the changing influence of the cycle counting algorithm can be observed in the results. Namely, the error variation already incorporated in profile #3 is not as much affected as profiles #1 and #2. The original signals for profiles #1 and #2 are smoother than profile #3 (cf. Figure 8), meaning that the implied error affects more, resulting in a greater difference with respect to the original damage estimation without errors. Figure 12 shows the extreme case of up to 30% error on the junction temperature T_j applied to the three different temperature profiles. As for negative error variations, the impact is negligible due to the exponential nature of $e_{T_{j,m}}$ in Eq. (7).

If the sum of the damage with errors is divided with the sum of the damage without errors in Figure 12, the last values shown in Figure 11 are obtained, that is 35.316 for profile #1, 26.5345 for profile #2 and 19.3758 for profile #3. Notice that these error terms are in relative units [cf. Eq. (8)].

4.2.2. Activation Time Uncertainty

The activation time is inferred from the duration of the cycles obtained from the rainflow cycle-count algorithm. The estimated activation time values are further post-processed including an error by repeating the uncertainty evaluation process. This stage is adopted at the end of the rainflow algorithm, so the cycle-count algorithm does not have an impact on the error quantification outcome. Figure 13 shows the impact of the activation time error on damage assessment.

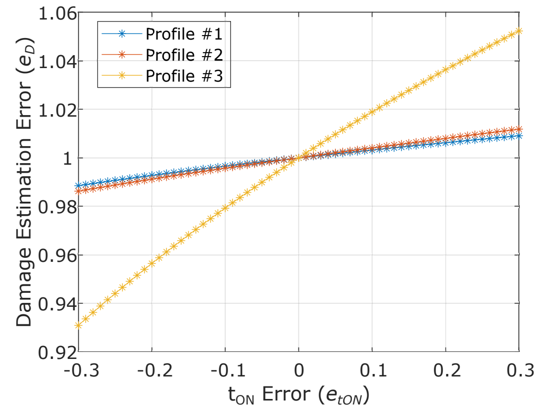

Figure 13. Effect of activation time error ($e_{T_{ON}}$) on damage estimation error (e_D).

It can be observed in Figure 13 that the damage estimation is sensitive to the errors in activation time. In this case, the most penalizing junction temperature profile #3 shows an increased damage estimation error. In contrast, junction temperature profiles #1 and #2 do not show a relevant impact on damage estimation error.

4.2.3. Uncertainty of the Constant Parameters

Subsequently, the uncertainty quantification process is applied to the constant parameters in Eq. (7). The errors in constant variable terms model the uncertainty associated with

the variable fitting process. Generally, constant variables are adjusted from experimental results, including the mean value and errors or residuals (Hernes et al., 2021). The error terms of constant variables in Eq. (7) denote this variation. Figure 14 shows the impact of the exponential error on the damage estimation.

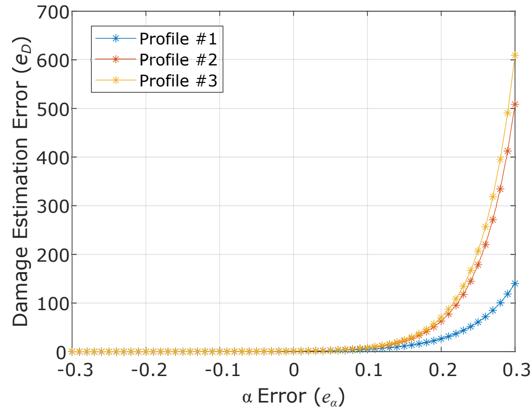

Figure 14. Effect of exponential parameter α error (e_α) on damage estimation error (e_D).

It can be observed in Figure 14 that the damage estimation is very sensitive to the errors in the exponential parameter, and it is directly related to the junction temperature. Namely, the higher the damage to the junction temperature, the higher is the effect on the damage estimation error. As for negative error variations, the impact is negligible due to the nature of e_α in Eq. (7).

Finally, for the constant error parameters, Figure 15 shows the effect on the damage estimation.

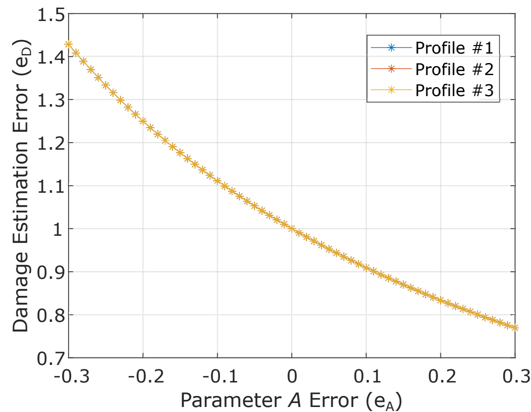

Figure 15. Effect of constant parameter A error (e_A) on damage estimation error (e_D).

It can be observed in Figure 15, that, the damage model is very sensitive to the errors in the constant parameter A. However, as opposed to previous cases, it can be observed that this is not dependent on the temperature, as this constant is an adaptation constant with no influence on the junction temperature.

4.2.4. Comparison of the Sources of Uncertainty

In order to cross-compare the different sources of uncertainty, Table 4 synthesizes the impact of the error of different variables on the damage estimation for the analysed profiles #1, #2 and #3. Note that each grid of the table is a normalized damage estimation with respect to the damage model without uncertainty, *i.e.* Table 4 synthesizes 120 normalized lifetime estimation error values.

All in all, it is observed that the most penalizing factor is the α parameter, due to its exponent impact on the damage. Among the rest of the parameters, it can be observed that the next most penalizing parameter is the T_j value. Both parameters show a direct relationship with a positive error causing an increase in the damage estimation error. However, it can be observed that there is the inverse effect as well, an increase in A leads to a decrease in the damage estimate. Finally, it can be concluded that the effect of the activation time error on the damage assessment is the least penalizing factor.

Among the tested junction temperature profiles, it can be observed that the higher the temperature, *i.e.* profile #3, the greater the impact on the damage estimation error of variable errors of α and t_{ON}. In contrast, the effect of the impact of the errors of T_j on damage estimation depend on the variations of the original T_j signal. Namely, the impact of the added uncertainties is greater when the original T_j signal has fewer cycles. In this case, the temperature profile #1 shows fewer variations than #3 (cf. Figure 8). However, when uncertainties are added, the resulting number of cycles are greater for the profile #1, and accordingly, the damage estimation error is higher. Finally, for the constant variable, A, the effect is constant across all the temperature profiles.

5. DISCUSSION

A practical conclusion of this research is the identification and ranking of the impact of the error of parameters and variables on the final lifetime estimation. Constant parameters that have been extracted from historic experimentation tests directly impact the lifetime assessment error. Namely, linear variations in α yield exponential lifetime assessment errors, while linear deviations in A lead to linear errors on lifetime assessment.

Similarly, junction temperature measurement errors impact negatively on the lifetime assessment. This indicates that a small measurement error, may be propagated and cause incorrect lifetime estimates. Finally, errors in activation time measurement are shown to be less relevant resulting in very mild differences in lifetime estimation.

Therefore, it is crucial to pay special attention to α and T_j

Table 4. Ordered damage error uncertainty for different parameters and for the profiles #1, #2 and #3 [%].

Error	α			T_j			A			t_{ON}		
	#1	#2	#3	#1	#2	#3	#1	#2	#3	#1	#2	#3
2%	38.3	52.6	52.5	33.9	30	27	-1.9	-1.9	-1.9	0.06	0.08	0.39
4%	91.6	127	130.6	77.6	70	61	-3.8	-3.8	-3.8	0.13	0.16	0.7
6%	165.9	243	255.6	133.4	118.8	102	-5.6	-5.6	-5.6	0.19	0.24	1.1
8%	269.5	418.9	443.7	204.1	179.4	151	-7.4	-7.4	-7.4	0.25	0.32	1.5
10%	409	685	731.9	293.1	254	211	-9.1	-9.1	-9.1	0.3	0.4	1.8
-2%	-27.6	-33.5	-34.1	-26.1	-24.4	-23	2.1	2.1	2.1	-0.06	-0.08	-0.4
-4%	-47.5	-55.7	-56.4	-45.9	-43	-40	4.1	4.1	4.1	-0.14	-0.17	-0.81
-6%	-61.8	-70	-71.2	-60.9	-58.1	-55	6.4	6.4	6.4	-0.21	-0.25	-1.3
-8%	-72.1	-80.3	-80.9	-72.1	-69.3	-66	8.7	8.7	8.7	-0.27	-0.34	-1.7
-10%	-79.6	-88	-88.3	-80.3	-78	-74	11.1	11.1	11.1	-0.34	-0.4	-2.1

values, as it has been observed that their impact on lifetime estimation is considerable.

It should be noted that the considered error variables have been considered in isolation, with no joint influence of uncertainties. This may be addressed in future research through probabilistic uncertainty modelling methods (H. Liu et al., 2021).

Uncertainty Modelling Alternatives

A conscious decision has been adopted to model the junction temperature uncertainty with a constant error, which provides traceability, and it is possible to estimate the impact of errors on the overall lifetime. In contrast, if non-constant error terms were adopted, these stochastic variations should then be post-processed through the rainflow algorithm. However, the relative thermal cycles estimated from the rainflow algorithm affects the error traceability, and consequently, the impact on overall lifetime estimation is lost.

Other error modelling alternatives were tested in this research so as to model the error term e_{T_j} in Eq. (6) including:

(i) a worst-case constant error term inferred from the maximum T_j value to each temperature value, $e_{T_j} = max(T_j) \times p$, where p is the error percentage. This results in offsetting the junction temperature signal, and in the end, cancelling the error effect in the rainflow counting algorithm.

(ii) a worst-case random error term inferred from the maximum T_j value to each temperature value, $e_{T_j} = max(T_j) \times R$, where $R = u[L, U]$ is a random uniform number specified in the limits between U and L, which are delimited by the error percentage p. This approach results in oscillations of the junction temperature signal, leading to counting multiple low temperature cycles.

Measurements for Validation

A more robust alternative to elicit the relationship between variable and uncertainty would require an extensive set of measurements, for which the design of new experimental campaigns is necessary (Štrbac et al., 2020).

A possible set of measurements may focus on repeated thermal measurements under different operation profiles and empirical inference of the underlying probability distribution of measurements (Górecki, Górecki, & Zarebski, 2019). This controlled measurement process would enable the characterization of measurement uncertainty, which includes calibration and quantization errors.

However, such experimental results are limited at the stage of the completion of this work. Therefore, this alternative is left as future work.

As for commercial modules, they may have been characterized with standard measurement practices and associated measurement errors. Accordingly, it is possible to use the proposed approach to infer the effect of the quoted error reference to infer the potential impact on damage estimation.

Generalization of the Proposed Approach

As for the generalization of the framework, the goal of this paper is to demonstrate how to include uncertainties on variables and assess their impact on lifetime error. The validity of the framework has been here demonstrated for SKiM63 modules based on empirical formulations validated in the literature. However, it is possible to apply the framework to other physical lifetime estimation models with different analytic formulations. To this end, the key constraint would be that the ageing process under study should be characterized by a cycling stress and a cumulative ageing process. Accordingly, the cycle count and cumulative ageing models would be applicable as outlined in Figure 5.

Fidelity of the Cycle Counting Algorithm

Finally, the fidelity and uncertainty of the cycle counting algorithm used to assess the damage of the junction temperature should be further examined. On the one hand, the adopted cycle counting process assumes that the bounds inferred from the rainflow algorithm correspond to individual thermal cy-

cles. However, if the nature of the junction temperature does not adhere to the underlying creep type mechanism adopted by the rainflow, e.g. long-lasting events, that may cause the bias of the counting process. On the other hand, the rainflow algorithm counts the cycles, but it does not take into account the order of events. This has a direct impact on lifetime estimation, as mild or severe cycles have a completely different impact on the IGBT lifetime. Similar concepts are evaluated in other reliability engineering areas through time-ordered models (Aizpurua, Papadopoulos, Muxika, Chiacchio, & Manno, 2017; Chiacchio, Aizpurua, D'Urso, & Compagno, 2018).

6. CONCLUSIONS

Insulated Gate Bipolar Transistors (IGBTs) are key semiconductor based power elements for various power-electronic systems. There are different failure modes associated with the lifetime of IGBTs. Focusing on the bond wire lift-off, it has been observed the lifetime models include a number of parameters that are prone to different sources of uncertainty. In this context, this research presents a methodology that enables the evaluation of the impact of the sources of uncertainty on lifetime and damage assessment. The uncertainty assessment process has been here applied to the SKiM63 module. However, it may be applicable to other modules with similar ageing mechanisms. However, for different physical lifetime models the ageing model may be different and, therefore, the approach may not be directly applicable. In these cases, it may be necessary to adapt the lifetime model in agreement with the underlying physical ageing process. This may include additional sources of uncertainty and different lifetime stress factors which need to be analyzed with respect to the damage estimation process.

Obtained results show that there are crucial parameters and variables, whose tiny error variations can imply a large impact on damage error estimation. Accordingly, developing sensing technology that reduces measurement errors associated to these variables directly contributes to the error reduction on IGBT lifetime estimation. Therefore, the present work demonstrates that it is important to consider these sources of uncertainty when estimating the IGBT lifetime.

Future lines may address the use of error measurements to limit the damage estimation error and extend the experiments with more extensive measurement campaigns.

ACKNOWLEDGEMENTS

J. I. Aizpurua is funded by the Ramón y Cajal Fellowship, Spanish State Research Agency (grant number RYC2022 - 037300 - I), co-funded by MCIU/AEI/10.13039/501100011033 and FSE+.

REFERENCES

Abuelnaga, A., Narimani, M., & Bahman, A. S. (2021). A review on igbt module failure modes and lifetime testing. *IEEE Access*, *9*, 9643-9663. doi: 10.1109/ACCESS.2021.3049738

Aizpurua, J. I., McArthur, S. D. J., Stewart, B. G., Lambert, B., Cross, J. G., & Catterson, V. M. (2019). Adaptive power transformer lifetime predictions through machine learning and uncertainty modeling in nuclear power plants. *IEEE Transactions on Industrial Electronics*, *66*(6), 4726-4737. doi: 10.1109/TIE.2018.2860532

Aizpurua, J. I., Papadopoulos, Y., Muxika, E., Chiacchio, F., & Manno, G. (2017). On cost-effective reuse of components in the design of complex reconfigurable systems. *Quality and Reliability Engineering International*, *33*(7), 1387-1406. doi: 10.1002/qre.2112

Aizpurua, J. I., Stewart, B. G., McArthur, S. D. J., Jajware, N., Kearns, M., Garro, U., ... Mendicute, M. (2021). A diagnostics framework for underground power cables lifetime estimation under uncertainty. *IEEE Transactions on Power Delivery*, *36*(4), 2014-2024. doi: 10.1109/TPWRD.2020.3017951

Antonopoulos, A., D'Arco, S., Hernes, M., & Peftitsis, D. (2019). Challenges and strategies for a real-time implementation of a rainflow-counting algorithm for fatigue assessment of power modules. In *2019 ieee applied power electr. conf. and expo.* (p. 2708-2713). doi: 10.1109/APEC.2019.8722284

Antonopoulos, A., D'Arco, S., Hernes, M., & Peftitsis, D. (2021). Limitations and guidelines for damage estimation based on lifetime models for high-power igbts in realistic application conditions. *IEEE Journal Emerging and Selected Topics in Power Electr.*, *9*(3), 3598-3609. doi: 10.1109/JESTPE.2020.3004093

ASTM. (2017). Standard Practices for Cycle Counting in Fatigue Analysis. *ASTM E1049-85*. doi: 10.1520/E1049-85R17

Bayerer, R., Herrmann, T., Licht, T., Lutz, J., & Feller, M. (2008). Model for power cycling lifetime of igbt modules - various factors influencing lifetime. In *5th int. conf. on integrated power electronics systems* (p. 1-6).

Cai, Y., Zhao, Y., Ma, X., & Zhou, K. (2020). Reliability assessment in dynamic field environment incorporating multiple environmental effects. *Proceedings of the Institution of Mechanical Engineers, Part O: Journal of Risk and Reliability*, *234*(1), 3-14. doi: 10.1177/1748006X19879607

Changcong, Z., Mengyao, J., Haodong, Z., & Fei, C. (2021). Uncertainty analysis of motion error for mechanisms and kriging-based solutions. *Proceedings of the Institution of Mechanical Engineers, Part O: Journal of Risk and Reliability*, *235*(5), 731-743. doi:

10.1177/1748006X21999019

Chiacchio, F., Aizpurua, J. I., D'Urso, D., & Compagno, L. (2018). Coherence region of the priority-and gate: Analytical and numerical examples. *Quality and Reliability Engineering International*, *34*(1), 107-115. doi: https://doi.org/10.1002/qre.2241

Degrenne, N., Ewanchuk, J., David, E., Boldyrjew, R., & Mollov, S. (2019). A prognostics framework for power semiconductor igbt modules through monitoring of the on-state voltage. In *Annual conference of the phm society* (Vol. 11). doi: 10.36001/phmconf.2019.v11i1.829

Degrenne, N., Kawahara, C., & Mollov, S. (2015). A review of prognostics and health management for power semiconductor modules. In *Annual conference of the phm society* (Vol. 7). doi: 10.36001/phmconf.2015.v7i1.2763

Elwakeel, A., Mcneill, N., Alzola, R. P., Surapaneni, R. K., Galla, G., Ybanez, L., … Yuan, W. (2023). Characterizing semiconductor devices for all-electric aircraft. *IEEE Access*, *11*, 73490-73504. doi: 10.1109/ACCESS.2023.3279088

Fu, J., Peyghami, S., Núñez, A., Blaabjerg, F., & De Schutter, B. (2023). A tractable failure probability prediction model for predictive maintenance scheduling of large-scale modular-multilevel-converters. *IEEE Transactions on Power Electronics*, 1-12. doi: 10.1109/TPEL.2023.3241317

Górecki, K., Górecki, P., & Zarebski, J. (2019). Measurements of parameters of the thermal model of the igbt module. *IEEE Transactions on Instrumentation and Measurement*, *68*(12), 4864-4875. doi: 10.1109/TIM.2019.2900144

Haque, M. S., Choi, S., & Baek, J. (2018). Auxiliary particle filtering-based estimation of remaining useful life of igbt. *IEEE Transactions on Industrial Electronics*, *65*(3), 2693-2703. doi: 10.1109/TIE.2017.2740856

Held, M., Jacob, P., Nicoletti, G., Scacco, P., & Poech, M.-H. (1997). Fast power cycling test of igbt modules in traction application. In *Proceedings of second international conference on power electronics and drive systems* (Vol. 1, p. 425-430 vol.1). doi: 10.1109/PEDS.1997.618742

Hernes, M., D'Arco, S., Antonopoulos, A., & Peftitsis, D. (2021). Failure analysis and lifetime assessment of igbt power modules at low temperature stress cycles. *IET Power Electr.*, *14*(7), 1271-1283. doi: https://doi.org/10.1049/pel2.12083

Huang, H., & Mawby, P. A. (2013). A lifetime estimation technique for voltage source inverters. *IEEE Transactions on Power Electronics*, *28*(8), 4113-4119. doi: 10.1109/TPEL.2012.2229472

Huang, Y., Luo, Y., Xiao, F., Liu, B., & Tang, X. (2023). Evaluation of the degradation in electrothermal characteristics of igbts during thermal cycling cocaused by solder cracking and al-wires lifting-off based on iterative looping. *IEEE Transactions on Power Electronics*, *38*(2), 1768-1778. doi: 10.1109/TPEL.2022.3209331

IEC. (2019). Semiconductor devices discrete devices. insulated-gate bipolar transistors (igbts). *IEC 60747-9*.

Infineon Technologies AG. (2013, 11). "IGBT modules – FF200R12KT4" [Computer software manual]. (Rev. 2.0)

Liu, H., Chen, M., Du, C., Tang, J., Fu, C., & She, G. (2021). A copula-based uncertainty propagation method for structures with correlated parametric p-boxes. *Int. J. Approximate Reasoning*, *138*, 89-104. doi: 10.1016/j.ijar.2021.08.002

Liu, J., Li, L., Chen, G., & Liu, Y. (2022). High precision igbt health evaluation method: Extreme learning machine optimized by improved krill herd algorithm. *IEEE Trans. Device and Materials Reliability*, 1-1. doi: 10.1109/TDMR.2022.3228253

Lu, Y., & Christou, A. (2017). Lifetime estimation of insulated gate bipolar transistor modules using two-step bayesian estimation. *IEEE Trans. Device and Materials Reliability*, *17*(2), 414-421. doi: 10.1109/TDMR.2017.2694158

Lutz, J., Schlangenotto, H., Scheuermann, U., & De Doncker, R. (2018). *Semiconductor power devices physics characteristics reliability (2nd ed. 2018).* Springer Int. Publishing. doi: 10.1007/978-3-319-70917-8

Mandeya, R., Chen, C., Pickert, V., & Naayagi, R. T. (2018). Prethreshold voltage as a low-component count temperature sensitive electrical parameter without self-heating. *IEEE Transactions on Power Electronics*, *33*(4), 2787-2791. doi: 10.1109/TPEL.2017.2749179

Matsuishi, M. (1968). Fatigue of metals subjected to varying stress. *Japan Society of Mechanical Engineers*.

Miner, M. A. (1945, 03). Cumulative Damage in Fatigue. *Journal of Applied Mechanics*, *12*(3), A159-A164. doi: 10.1115/1.4009458

Qin, F., Bie, X., An, T., Dai, J., Dai, Y., & Chen, P. (2021). A lifetime prediction method for igbt modules considering the self-accelerating effect of bond wire damage. *IEEE Journal of Emerging and Selected Topics in Power Electronics*, *9*(2), 2271-2284. doi: 10.1109/JESTPE.2020.2992311

Scheuermann, U., & Schmidt, R. (2013). Impact of load pulse duration on power cycling lifetime of al wire bonds. *Microelectronics Reliability*, *53*(9), 1687-1691. doi: 10.1016/j.microrel.2013.06.019

Trespaderne, D. A. (2016). *Design and implementation of a prognostic and health monitoring system for the power electronics converter of a fev powertrain* (Unpublished doctoral dissertation). Universidad de Navarra.

Tu, C., Xu, H., Xiao, B., Lu, J., Guo, Q., & Long, L. (2022). Research on the influence of bond wire lift-off posi-

tion on the electro-thermal characteristics of igbt. *IEEE Transactions on Electron Devices*, *69*(3), 1271-1278. doi: 10.1109/TED.2022.3140689

Yang, S., Xiang, D., Bryant, A., Mawby, P., Ran, L., & Tavner, P. (2010). Condition monitoring for device reliability in power electronic converters: A review. *IEEE Trans. Power Electr.*, *25*(11), 2734-2752. doi: 10.1109/TPEL.2010.2049377

Yaqub, I., Li, J., & Johnson, C. M. (2015). Dependence of overcurrent failure modes of igbt modules on interconnect technologies. *Microelectronics Reliability*, *55*(12, Part A), 2596-2605. doi: 10.1016/j.microrel.2015.09.020

Štrbac, B., Ačko, B., Havrlišan, S., Matin, I., Savković, B., & Hadžistević, M. (2020). Investigation of the effect of temperature and other significant factors on systematic error and measurement uncertainty in cmm measurements by applying design of experiments. *Measurement*, *158*, 107692. doi: 10.1016/j.measurement.2020.107692